Supporting Information

Self-Supported FeP Nanorod Arrays: A Cost-Effective 3D Hydrogen Evolution Cathode with High Catalytic Activity

Yanhui Liang,[†] Qian Liu,[†] Abdullah M. Asiri,[§,‖] Xuping Sun,[†,§,‖*] and Yonglan Luo[†*]

[†] Chemical Synthesis and Pollution Control Key Laboratory of Sichuan Province, College of Chemistry and Chemical Engineering, China West Normal University, Nanchong 637002, Sichuan, China

[§] Center of Excellence for Advanced Materials Research, King Abdulaziz University, Jeddah 21589, Saudi Arabia

[‖] Chemistry Department, Faculty of Science, King Abdulaziz University, Jeddah 21589, Saudi Arabia

*E-mail: sunxp@cwnu.edu.cn; luoylcwnu@hotmail.com

Experimental Section

Materials

NaH_2PO_2 was purchased from Aladdin Ltd. (Shanghai, China). $FeCl_3 \cdot 6H_2O$, Na_2SO_4 and HNO_3 were purchased from Beijing Chemical Corporation. CC was provided by Hongshan District, Wuhan Instrument Surgical Instruments business. Pt/C was purchased from Sigma-Aldrich. All chemicals were used as received without further purification.

Preparation of Fe_2O_3 NAs/CC

Typically, CC was carefully cleaned with concentrated HNO_3 to remove impurity of surface, and then deionized water and ethanol were used for several times to ensure the surface of the CC was well cleaned. A 35 ml aqueous containing 0.4 g $FeCl_3 \cdot 6H_2O$ and 0.24 g Na_2SO_4 was stirred for 10 min, and then transferred to a 50 mL Teflon-lined stainless-steel autoclave. Afterwards, the dried CC (2 cm × 3 cm) was immersed into the solution and hydrothermally treated at 120 ºC for 6 h and then cool down to ambient atmosphere. Finally, the Fe_2O_3 NAs/CC was obtained after annealing in Ar gas at 450 ºC for 3 h.

Preparation of FeP NAs/CC

Fe_2O_3 NAs/CC and NaH_2PO_2 were placed at two separate positions in one closed porcelain crucible with NaH_2PO_2 at the upstream side of the furnace. Subsequently, the samples were heated at 300 ℃ for 2 h with a heating speed of 2 ℃/min in Ar atmosphere. After that, FeP NAs/CC was collected after cooled to ambient temperature under Ar atmosphere. The loading for FeP on CC was determined to be ~1.5 mg/cm^2.

Characterizations

Powder XRD data were acquired on a RigakuD/MAX 2550 diffractometer with Cu Kα radiation (λ=1.5418 Å). SEM measurements were carried out on a XL30 ESEM FEG scanning electron microscope at an accelerating voltage of 20 kV. TEM measurements were performed on a HITACHI H-8100 electron microscopy (Hitachi, Tokyo, Japan) with an accelerating voltage of 200 kV. XPS measurements were performed on an ESCALABMK II X-ray photoelectron spectrometer using Mg as the exciting source. The generated gas was confirmed by gas chromatography (GC) analysis and measured quantitatively using a calibrated pressure sensor to monitor the pressure change in the cathode compartment of a H-type electrolytic cell. The Faradaic efficiency was calculated by comparing the amount of measured hydrogen generated by potentiostatic cathodic electrolysis with calculated hydrogen (assuming 100% Faradaic efficiency). The rough agreement of both values suggests nearly 100% Faradaic efficiency. GC analysis was carried out on GC–2014C (Shimadzu Co.) with thermal conductivity detector and nitrogen carrier gas. Pressure data during electrolysis were recorded using a CEM DT-8890 Differential Air Pressure Gauge Manometer Data Logger Meter Tester with a sampling interval of 1 point per second.

Electrochemical measurements

All the electrochemical measurements were conducted using a CHI660E potentiostat (CH Instruments, China) in a typical three-electrode setup with an electrolyte solution of 0.5 M H_2SO_4, a graphite rod as the counter electrode and a saturated calomel electrode (SCE) as the reference electrode. IR correction was determined using electrochemical impedance measurements. In all measurements, the SCE reference electrode was calibrated with respect to reversible hydrogen electrode (RHE). Linear sweep voltammetrys (LSVs) was conducted in 0.5 M H_2SO_4 with scan rate of 2 mV/s. Onset overpotential was determined

based on the beginning of linear regime in the Tafel plot. All the potentials reported in our work were vs. the RHE. The RHE calibration was carried out in highly pure hydrogen saturated electrolyte with a Pt foil as the working electrode according to reported method.[1] Cyclic voltammetry was run at a scan rate of 1 mV/s, and the average of the two potentials at which the current crossed zero was taken to be the thermodynamic potential for the hydrogen electrode reaction. In 0.5 M H_2SO_4, E (RHE) = E (SCE) + 0.281 V. In 1 M PBS, E (RHE) = E (SCE) + 0.655 V. In 1M KOH, E (RHE) = E (SCE) + 1.068 V.

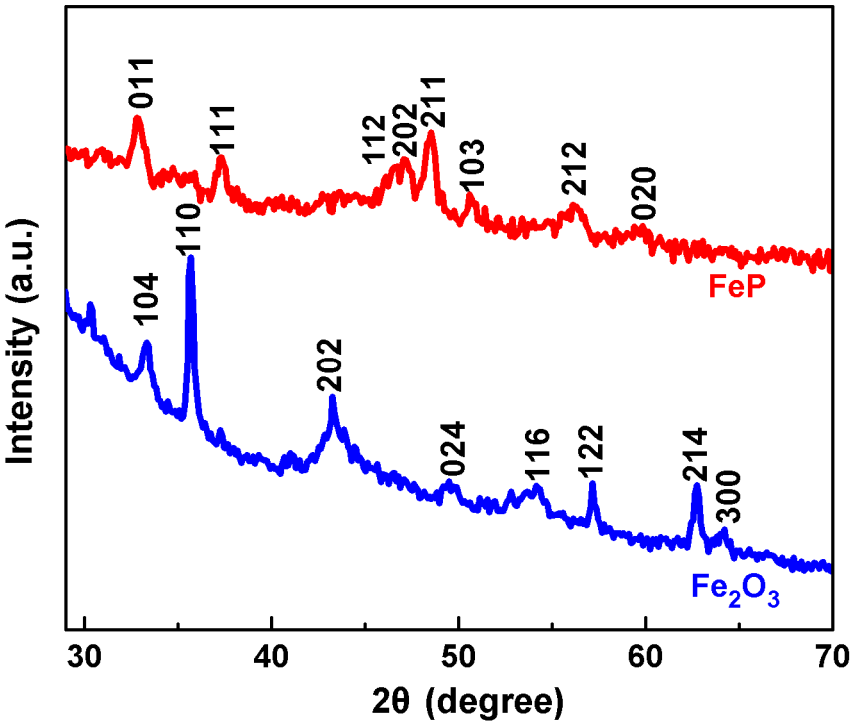

Figure S1. XRD patterns for Fe_2O_3 and FeP scratched from CC.

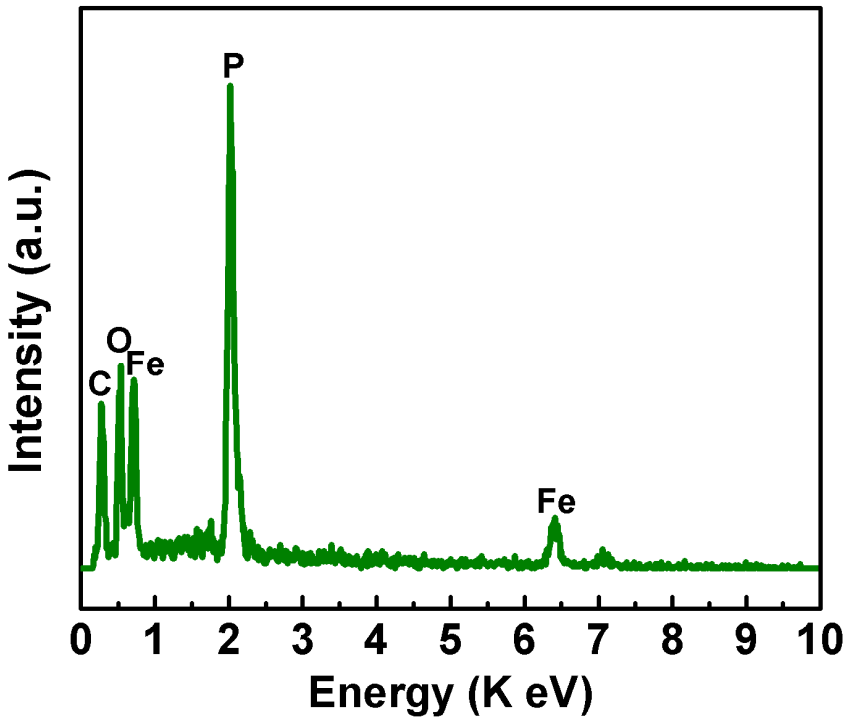

Figure S2. EDX spectrum of FeP NAs/CC.

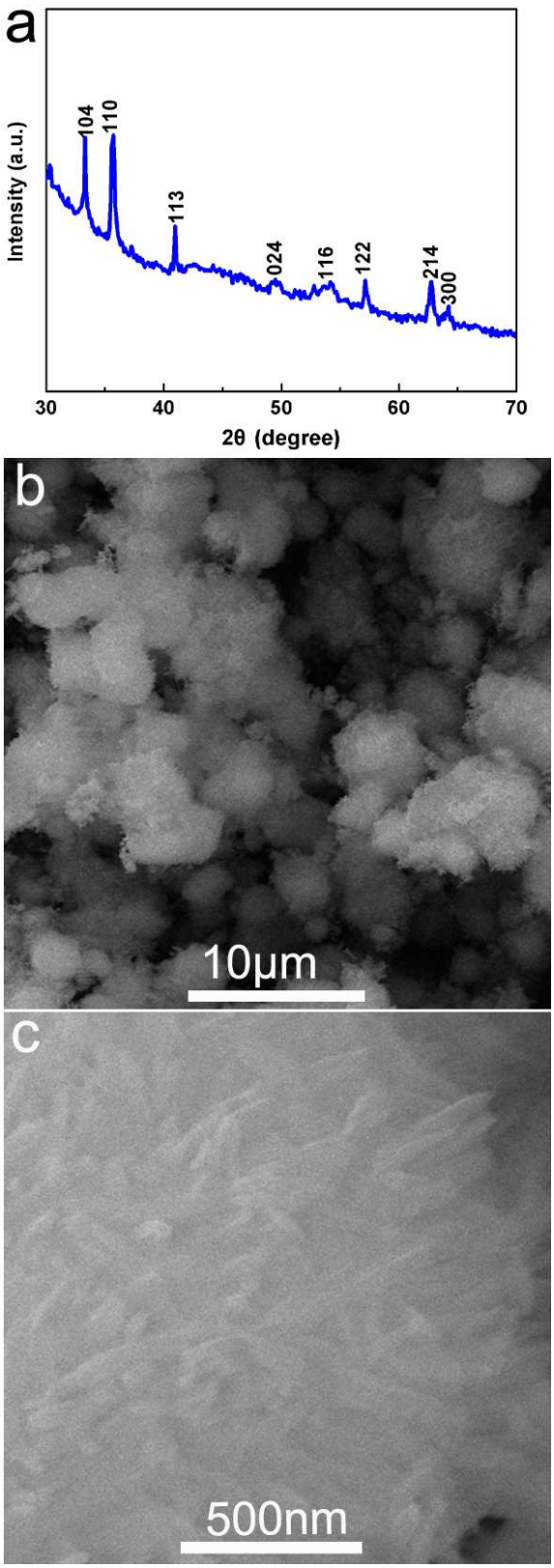

Figure S3. (a) XRD pattern and (b, c) SEM images of Fe_2O_3 MPs.

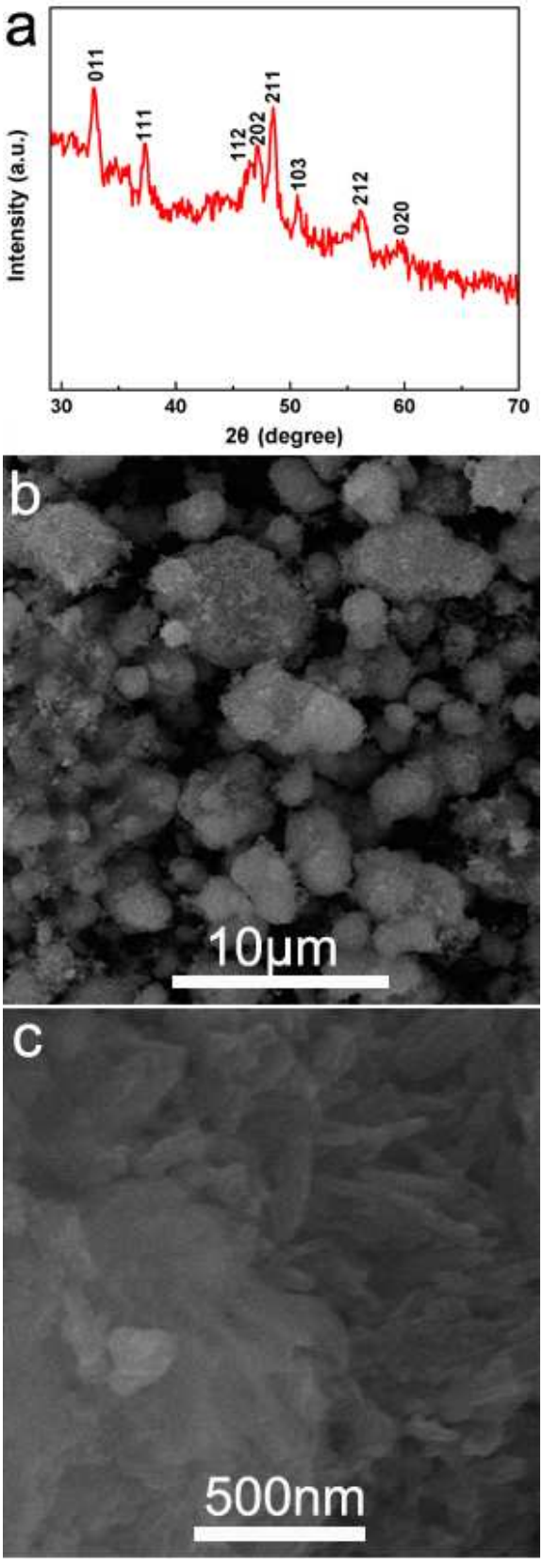

Figure S4. (a) XRD pattern and (b, c) SEM images of FeP MPs.

Table S1. Comparison of HER performance in acidic electrolytes for FeP NAs/CC with other non-noble-metal HER electrocatalysts ([a] catalysts directly grown on current collectors).

Catalyst	Current density (j, mA/cm^2)	η at the corresponding j (mV)	Exchange current density (mA/cm^2)	Ref
$CoSe_2$ NP/CP[a]	10	139	$(4.9\pm1.4)\times10^{-3}$	2
double-gyroid MoS_2/FTO[a]	2	190	6.9×10^{-4}	3
metallic MoS_2 nanosheets	10	195	-	4
defect-rich MoS_2	13	200	8.91×10^{-3}	5
MoS_2/graphene/Ni foam[a]	10	141	-	6
MoO_3-MoS_2/FTO[a]	10	310	8.2×10^{-5}	7
bulk Mo_2C	1	~150	1.3×10^{-3}	8
bulk MoB	1	~150	1.4×10^{-3}	8
MoN/C	2	290	3.6×10^{-2}	9
Mo_2C/CNT	10	152	0.014	10
$NiMoN_x$/C	5	220	0.24	12
$Co_{0.6}Mo_{1.4}N_2$	10	200	0.23	13
Ni_2P hollow nanoparticles	10	116	0.033	14
Ni_2P nanoparticles	20	140	-	15
CoP nanoparticles	20	85	0.14	16
CoP nanotubes	10	144	-	17
CoP nanowires	10	110	0.15	18
CoP/CNT	10	122	0.13	19
CoP/CC[a]	10	67	0.29	20
Cu_3P NWs/CF[a]	10	143	0.18	21
interconnected network of MoP nanoparticles	10	125	0.086	22
bulk MoP	30	180	0.034	23
amorphous MoP nanoparticles	10	90	0.12	24
amorphous WP nanoparticles	10	120	-	25
FeP nanosheets	10	~240	-	26
FeP nanowire array/Ti[a]	10	55	0.42	27
FeP nanorod arrays/Ti[a]	10	85	-	28
FeP NAs/CC[a]	10	58	0.50	This work

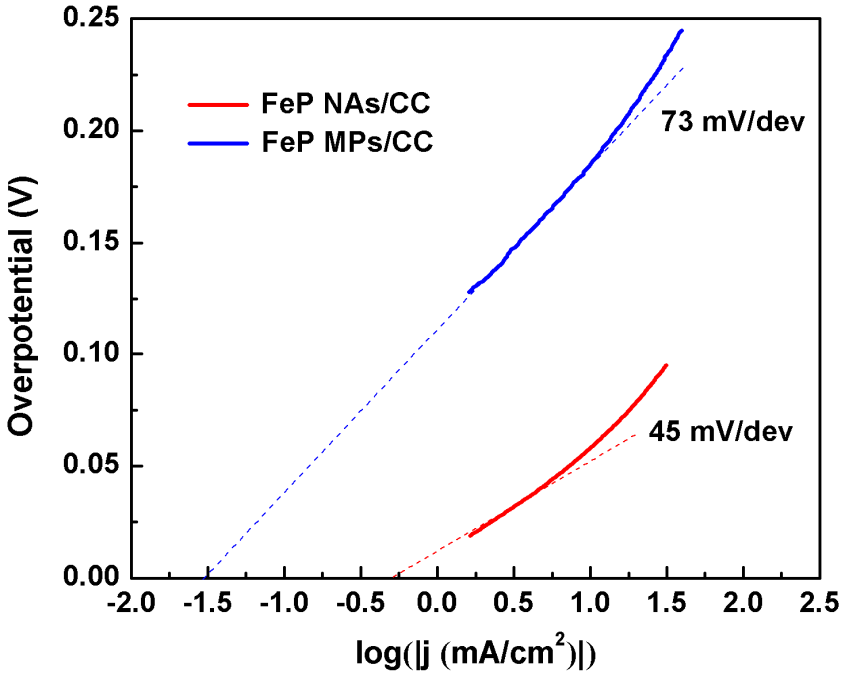

Figure S5. Calculation of exchange current density of FeP NAs/CC and FeP MPs/CC.

The exchange current density (j_0) was calculated using extrapolation methods. When the overpotential value is 0, the log[j] values for FeP NAs/CC and FeP MPs/CC are -0.3 and -1.53, respectively. Based on Tafel equations, j_0 for FeP NAs/CC and FeP MPs/C*C* was calculated to be 0.50 and 0.03 mA/cm^2, respectively.

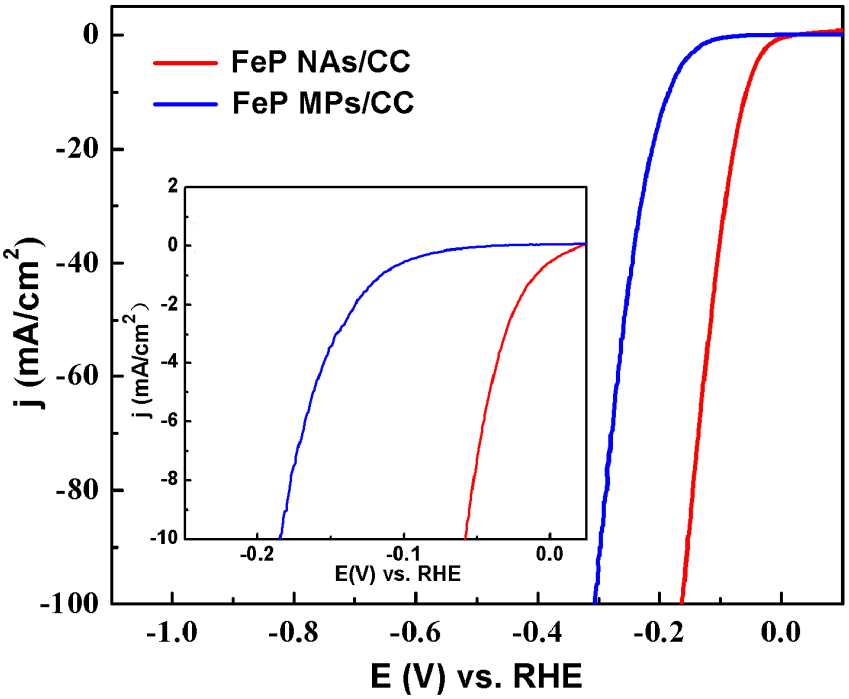

Figure S6. Polarization curves for FeP NAs/CC and FeP MPs/CC in 0.5 M H_2SO_4 with a scan rate of 2 mV/s.

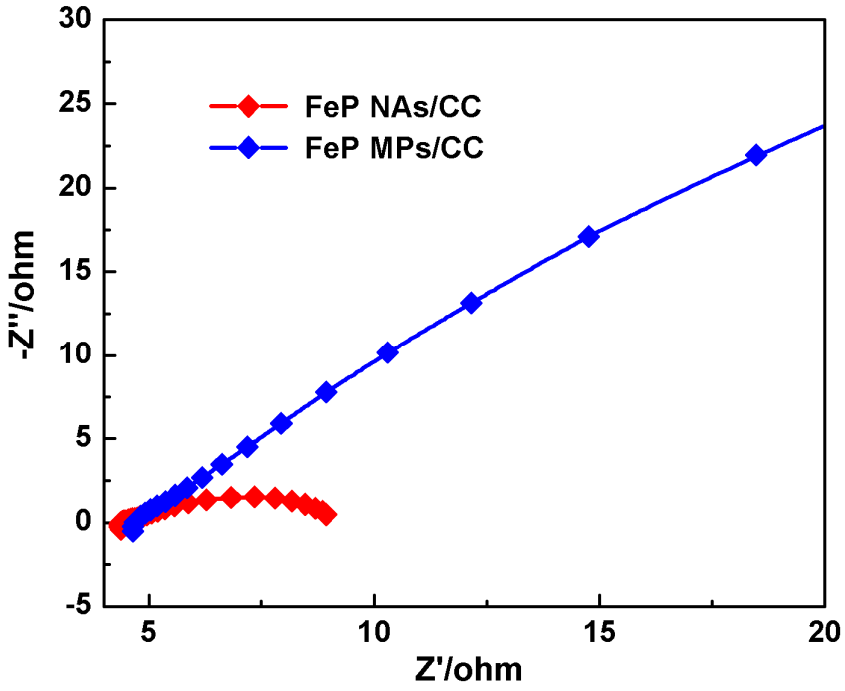

Figure S7. Nyquist plots of FeP NAs/CC and FeP MPs/CC recorded at η = 100 mV in 0.5 M H_2SO_4 solution.

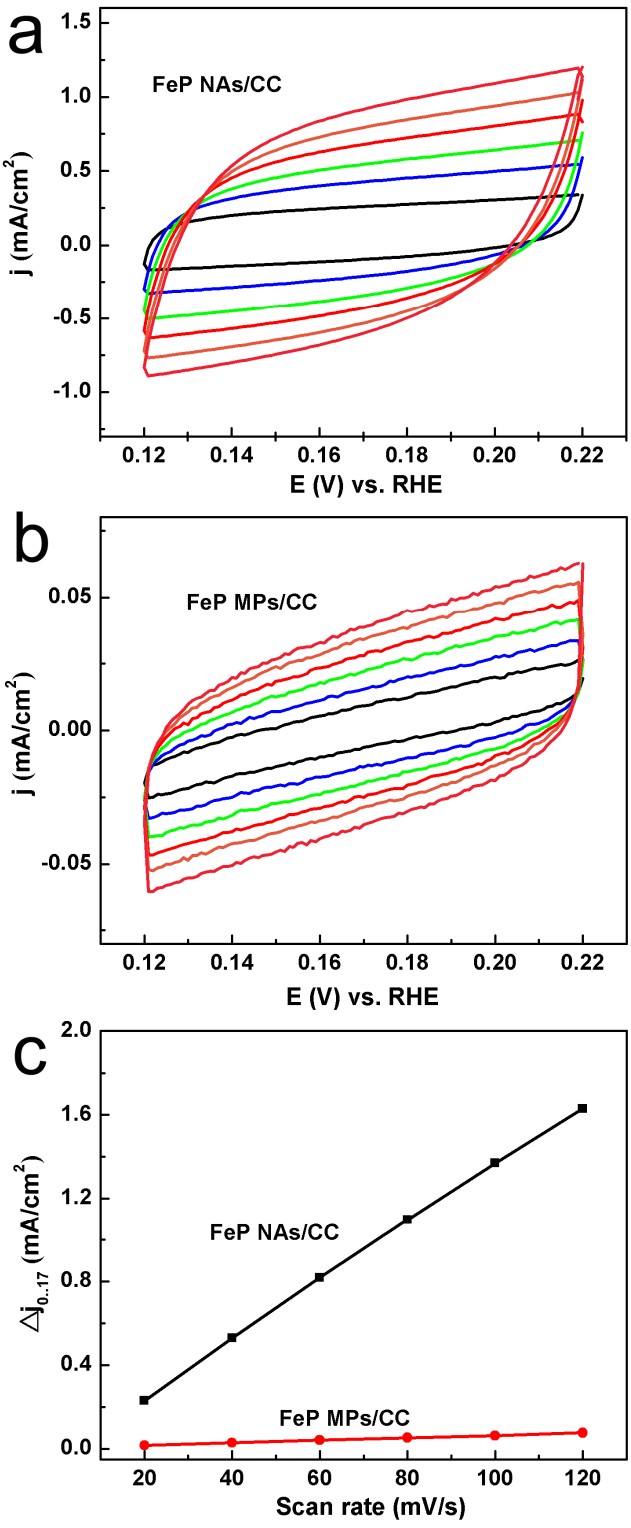

Figure S8. Cyclic voltammetrys for (a) FeP NAs/CC and (b) FeP MPs/CC. (c) The capacitive currents at 0.17 V as a function of scan rate for FeP NAs/CC and FeP MPs/CC

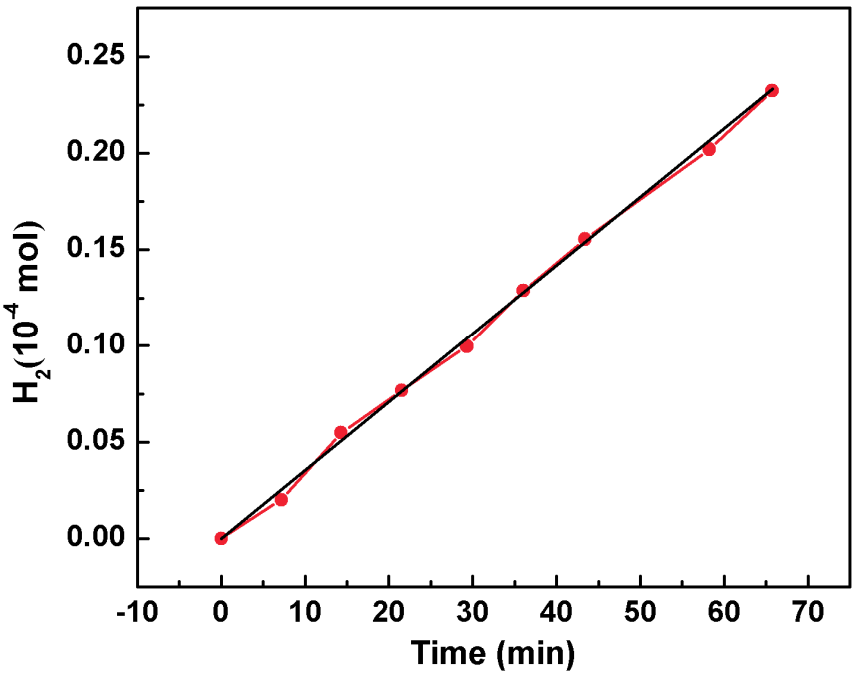

Figure S9. The amount of theoretically calculated (solid) and experimentally measured (square) hydrogen versus time for FeP NAs/CC for 70 min.

Table S2. Comparison of HER performance in neutral electrolytes for FeP NAs/CC with other non-noble-metal HER electrocatalysts ([a] catalysts directly grown on current collectors).

Catalyst	Current density (*j*, mA cm^{-2})	Overpotential at the corresponding *j* (mV)	Ref
bulk Mo_2C	1	200	8
bulk Mo_2B	1	250	8
Co-NRCNTs	2	380	13
	10	540	
CoP/CC[a]	2	65	20
H_2-CoCat/FTO[a]	2	385	29
Co-S/FTO[a]	2	83	30
FeP NAs/CC[a]	1	113	This work
	10	202	

Table S3 Comparison of HER performance in alkaline media for FeP NAs/CC with other non-noble-metal HER electrocatalysts ([a] catalysts directly grown on current collectors).

Catalyst	Current density (j, mA cm^{-2})	Overpotential at the corresponding j (mV)	Ref.
bulk MoB	10	225	8
Ni	10	400	8
Co-NRCNTs	1	160	13
	10	370	
Ni_2P nanoparticles	20	250	16
CoP/CC[a]	1	115	20
	10	209	
Co-S/FTO[a]	1	480	30
amorphous MoS_2/FTO[a]	10	540	31
Ni-Mo alloy/Ti foil[a]	10	80	32
Ni wire	10	350	32
FeP NAs/CC[a]	10	218	This work

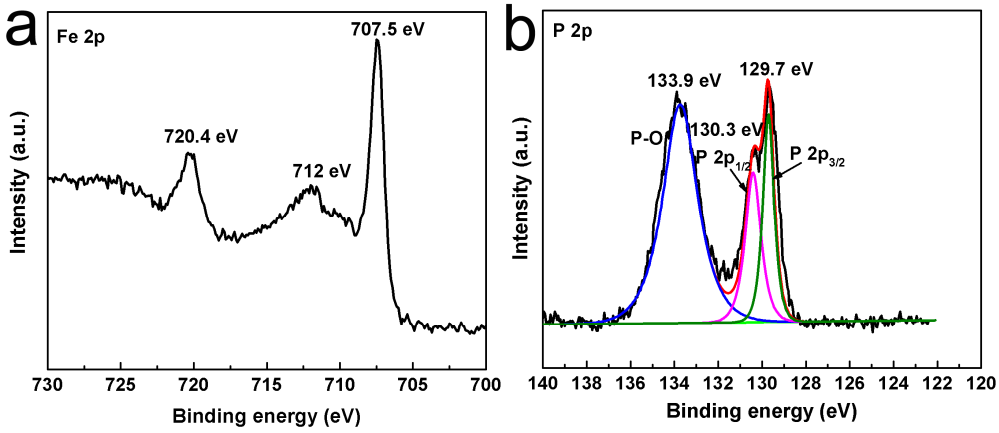

Figure S10. XPS spectra in the (a) Fe(2p) and (b) P(2p) regions for FeP NAs/CC.

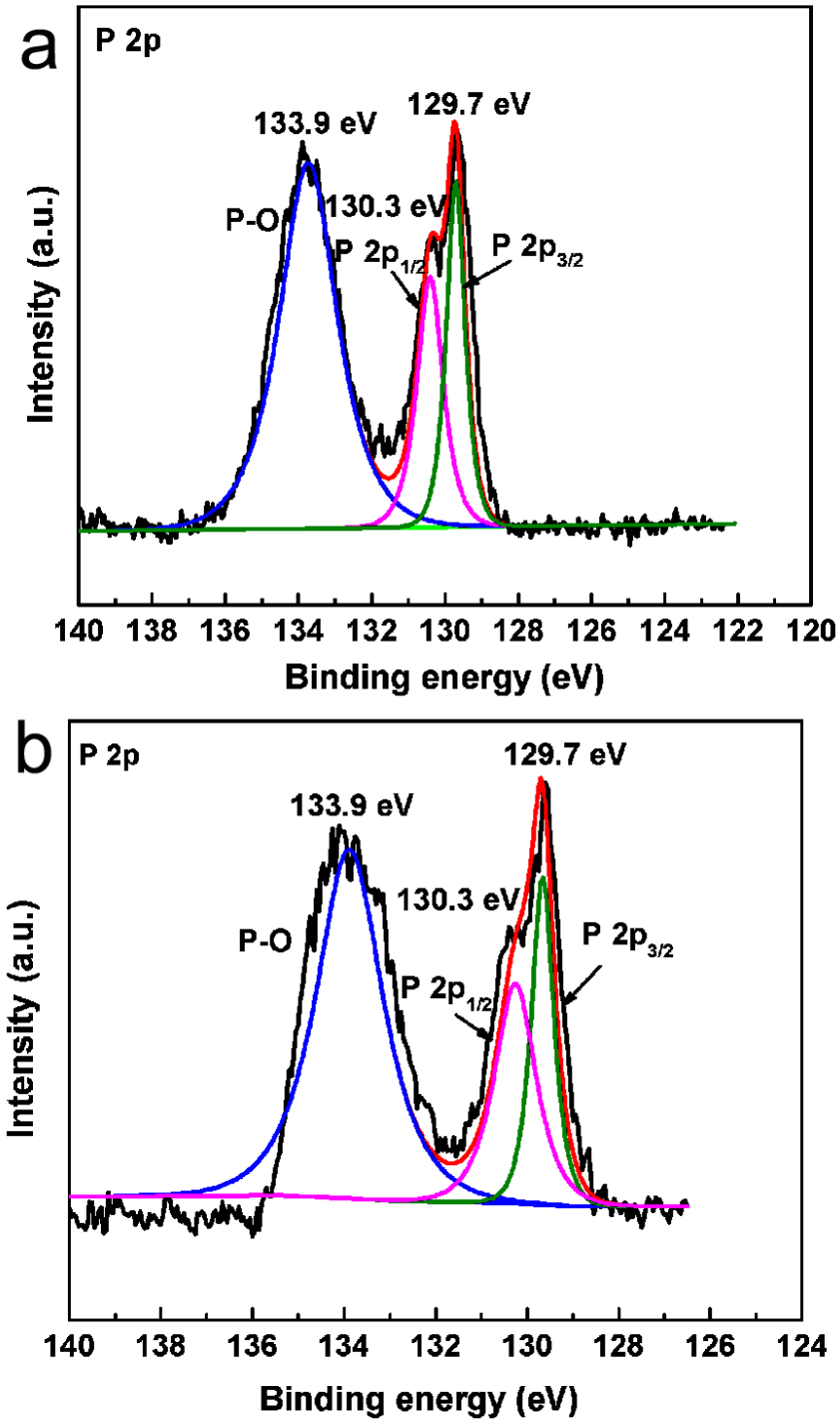

Figure S11. XPS spectra in the P(2p) region for FeP NAs/CC (a) before and (b) after electrolysis. This FeP catalyst shows similar numeric area of P(2p) region before (18530 CPS. eV) and after (17650 CPS. eV) electrolysis, implying the form of active catalyst is not changed by electrochemical experiments.

References

1 Xu, Y.; Gao, M.; Zheng, Y; Jiang, J; Yu, S. *Angew. Chem. Int. Ed.* **2013**, *52*, 8546–8550.
2 Kong, D.; Wang, H.; Lu, Z.; Cui, Y. *J. Am. Chem. Soc.* **2014**, *136*, 4897–4900.
3 Kibsgaard, J.; Chen, Z.; Reinecke, B. N.; Jaramillo, T. F. *Nat. Mater.* **2012**, *11*, 963–969.
4 Lukowski, M. A.; Daniel, A. S.; Meng, F.; Forticaux, A.; Li, L.; Jin, S. *J. Am. Chem. Soc.* **2013**, *135*, 10274–10277.
5 Xie, J.; Zhang, H.; Li, S.; Wang, R.; Sun, X.; Zhou, M.; Zhou, J.; Lou, X.; Xie, Y. *Adv. Mater.* **2013**, *25*, 5807–5813.
6 Chang, Y.; Lin, C.; Chen, T.-Y.; Hsu, C.-L.; Lee, Y.-H.; Zhang, W.; Wei, K.-H.; Li, L.-J. *Adv. Mater.* **2013**, *25*, 756–760.
7 Chen, Z.; Cummins, D.; Reinecke, B. N.; Clark, E.; Sunkara, M. K.; Jaramillo, T. F. *Nano Lett.* **2011**, *11*, 4168–4175.
8 Vrubel, H.; Hu, X. *Angew. Chem. Int. Ed.* **2012**, *54*, 12703–12706.
9 Chen, W.; Sasaki, K.; Ma, C.; Frenkel, A. I.; Marinkovic, N.; Muckerman, J. T.; Zhu, Y.; Adzic, R. R. *Angew. Chem. Int. Ed.* **2012**, *51*, 6131–6135.
10 Chen, W.; Wang, C.; Sasaki, K.; Marinkovic, N.; Xu, W.; Muckerman, J. T.; Zhu, Y.; Adzic, R. R. *Energy Environ. Sci.* **2013**, *6*, 943–951.
11 Chen, W.; Sasaki, K.; Ma, C.; Frenkel, A. I.; Marinkovic, N.; Muckerman, J. T.; Zhu, Y.; Adzic, R. R. *Angew. Chem. Int. Ed.* **2012**, *51*, 6131–6135.
12 Cao, B.; Veith, G. M.; Neuefeind, J. C.; Adzic, R. R.; Khalifah, P. G. *J. Am. Chem. Soc.* **2013**, *135*, 19186–19192.
13 Zou, X.; Huang, X.; Goswami, A.; Silva, R.; Sathe, B. R.; Mikmeková, E.; Asefa, T. *Angew. Chem. Int. Ed.* **2014**, 53, 4372–4376.
14 Popczun, E. J.; McKone, J. R.; Read, C. G.; Biacchi, A. J.; Wiltrout, A. M.; Lewis, N. S.; Schaak, R. E. *J. Am. Chem. Soc.* **2013**, *135*, 9267–9270
15 Feng, L.; Vrubel, H.; Bensimon, M.; Hu, X. *Phys. Chem. Chem. Phys.* **2014**, *16*, 5917–5921.
16 Popczun, E. J.; Read, C. G.; Roske, C. W.; Lewis, N. S.; Schaak, R. E. *Angew. Chem. Int. Ed.* **2014**, *53*, 5427–5430.
17 Du, H.; Liu, Q.; Cheng, N.; Asiri, A. M.; Sun, X.; Li, C. M. *J. Mater. Chem. A*, 2014, **2**, 14812–14816.
18 Jiang, P.; Liu, Q.; Ge, C.; Cui, W.; Pu, Z.; Asiri, A. M.; Sun, X. *J. Mater. Chem. A* **2014**, *2*, 14634–14640
19 Liu, Q.; Tian, J.; Cui, W.; Jiang, P.; Cheng, N.; Asiri, A. M.; Sun, X. *Angew. Chem. Int. Ed.* **2014**, *53*, 6710–6714.
20 Tian, J.; Liu, Q.; Asiri, A. M.; Sun, X. *J. Am. Chem. Soc.* **2014**, *136*, 7587–7590.
21 Tian, J.; Liu, Q.; Cheng, N.; Asiri, A. M.; Sun, X. *Angew. Chem. Int. Ed.* **2014**, *53*, 9577–9581
22 Xing, Z.; Liu, Q.; Asiri, A. M.; Sun, X. *Adv. Mater.* **2014**, *26*, 5702–5707.
23 Xiao, P.; Sk, M. A.; Thia, L.; Ge, X.; Lim, R. J.; Wang, J.; Lim, K. H.; Wang, X. *Energy Environ. Sci.* **2014**, *7*, 2624–2629
24 McEnaney, J. M.; Crompton, J. C.; Callejas, J. F.; Popczun, E. J.; Biacchi, A. J.; Lewis, N. S.; Schaak, R. E. *Chem. Mater.* **2014**, *26*, 4826–4831.
25 McEnaney, J. M.; Crompton, J. C.; Callejas, J. F.; Popczun, E. J.; Read, C. G.; Lewis, N. S.; Schaak, R. E. *Chem. Commun.* **2014**, *50*, 11026–11028.
26 Xu, R.; Wu, R.; Zhang, J.; Shi, Y.; Zhang, B. *Chem. Commun.* **2013**, *49*, 6656–6658.
27 Jiang, P.; Liu, Q.; Liang, Y.; Tian, J.; Asiri, A. M.; Sun, X. *Angew. Chem. Int. Ed.* DOI: 10.1002/anie.201406848.
28 Liu, R.; Gu, S.; Du, H.; Li, C. M. *J. Mater. Chem. A* **2014**, *2*, 17263–17267.
29 Cobo, S.; Heidkamp, J.; Jacques, P.-A.; Fize, J.; Fourmond, V.; Guetaz, L.; Jousselme, B.; Ivanova, V.; Dau, H.; Palacin, S.; Fontecave, M.; Artero, V. *Nat. Mater.* **2012**, *11*, 802-807.
30 Sun, Y.; Chong, L.; Grauer, D. C.; Yano, J.; Long, J. R.; Yang, P.; Chang, C. J. *J. Am. Chem. Soc.* **2013**, *135*, 17699-17702.

31 Merki, D.; Fierro, S.; Vrubel, H.; Hu, X. *Chem. Sci.* **2011**, *2*, 1262-1267.
32 McKone, J. R.; Sadtler, B. F.; Werlang, C. A.; Lewis, N. S.; Gray, H. B. A*CS Catal.* **2013**, *3*, 166-169.